UNIVERSITY OF
BATH

Citation for published version:
Salmon, P & Huang, L 2017, 'Impact of pressure on the structure of glass and its material properties', MRS Bulletin, vol. 42, no. 10, pp. 734-737. https://doi.org/10.1557/mrs.2017.210

DOI:
10.1557/mrs.2017.210

Publication date:
2017

Document Version
Peer reviewed version

[Link to publication](#)

University of Bath

IMPACT OF PRESSURE ON THE STRUCTURE OF GLASS AND ITS MATERIAL PROPERTIES

Philip S. Salmon[a] and Liping Huang[b]

[a]Department of Physics, University of Bath, Bath BA2 7AY, UK
[b]Department of Materials Science and Engineering, Rensselaer Polytechnic Institute, Troy, NY 12180, USA

High pressures have a significant impact on the structure-related properties of glass, and are encountered in scenarios that range from fracture mechanics, where stress in the gigapascal regime is easily generated by sharp-contact loading, to the manufacture of permanently densified materials with tuned physical characteristics. Here, we consider the pressure-induced structural changes that occur in glass and show that, for oxide materials, the oxygen-packing fraction plays a key role in determining when these changes are likely to occur. Fivefold coordinated Si atoms appear as important intermediaries in the pressure-induced deformation of silica glass.

Key Words: amorphous, oxide, densification, elastic properties, nano-indentation, simulation, structural

Introduction

The structure-related physical properties of glassy materials can be changed significantly by the application of pressure,[1–9] making it an important parameter for processing and characterisation in glass science and engineering. It is therefore important to understand the mechanisms of compaction, which can be either gradual or abrupt as in so-called polyamorphic transformations.[10,11] Unravelling the nature of structural change is, however, a formidable task because of the complexity that originates from the atomic-scale disorder of glass, and the experimental difficulties that are associated with the *in situ* investigation of materials under extreme conditions.[12] Nevertheless, the combination of experiment with modern modelling methods is beginning to reveal the structure and related properties of glassy materials at high pressure.[9,13]

In the following, silica glass will be used as an exemplar because it is the basic constituent of silicate materials, and there is much information on its pressure-dependent structure and properties from both experiment and computer simulation. Here, it is important to realise that the force applied in an experiment will not induce pure normal stress, unless a pressure transmitting medium is employed to give hydrostatic conditions. More generally, the force acting on a surface will have components that are both perpendicular and parallel to that surface, thus inducing normal and shear stresses, respectively. The resultant deformation is either elastic or plastic, depending on whether or not the material returns to its original shape when the load is removed.

<u>Why is pressure important for glass?</u>

Stress in the gigapascal regime is easily generated at the surface of glass by sharp-contact loading as in a Vickers hardness test, or when a sharp tip is moved laterally to induce a scratch.[14] Material with an ability to resist surface deformation is a highly desirable characteristic for applications that include the cover glass for electronic devices, high pressure windows, and glass for security and safety purposes. A successful strategy for strengthening the surface of glass is to place it under "chemical pressure." Here, an ion exchange (IOX) process involving a molten salt is used to replace, e.g., the smaller Na^+ cations in the surface region of a sodium aluminosilicate glass by larger K^+ cations.[15-17] In this way, the surface is placed under a compressive stress that can be ≥ 0.5 GPa. It is also desirable for glass to have a high fracture toughness, i.e., an ability to resist fracturing once a crack is formed via the suppression of crack propagation. The impact of high pressure on the structure of glass and its related material properties is therefore of key importance for understanding the fundamentals of fracture mechanics at an atomistic level.

The properties of glass can be tuned by using pressure to induce permanent densification, as illustrated in **Figure 1**a-b for the bulk modulus and Poisson's ratio (ν) of vitreous SiO_2.[7,9] Here, a compacted material is recovered to ambient conditions, and the extent of densification can be controlled via the choice of pressure and temperature treatment. The structural relaxation times are sufficiently long for the glass to be regarded as permanently densified. Experiment shows that the extent of permanent densification in different types of glass is related to ν, defined as the negative of the ratio of transverse contraction strain to longitudinal extension strain in the direction of elastic loading. This dependence reflects the underlying atomic structure of the material as measured by the atomic packing density C_g, where more open network structures have smaller C_g values.[18]
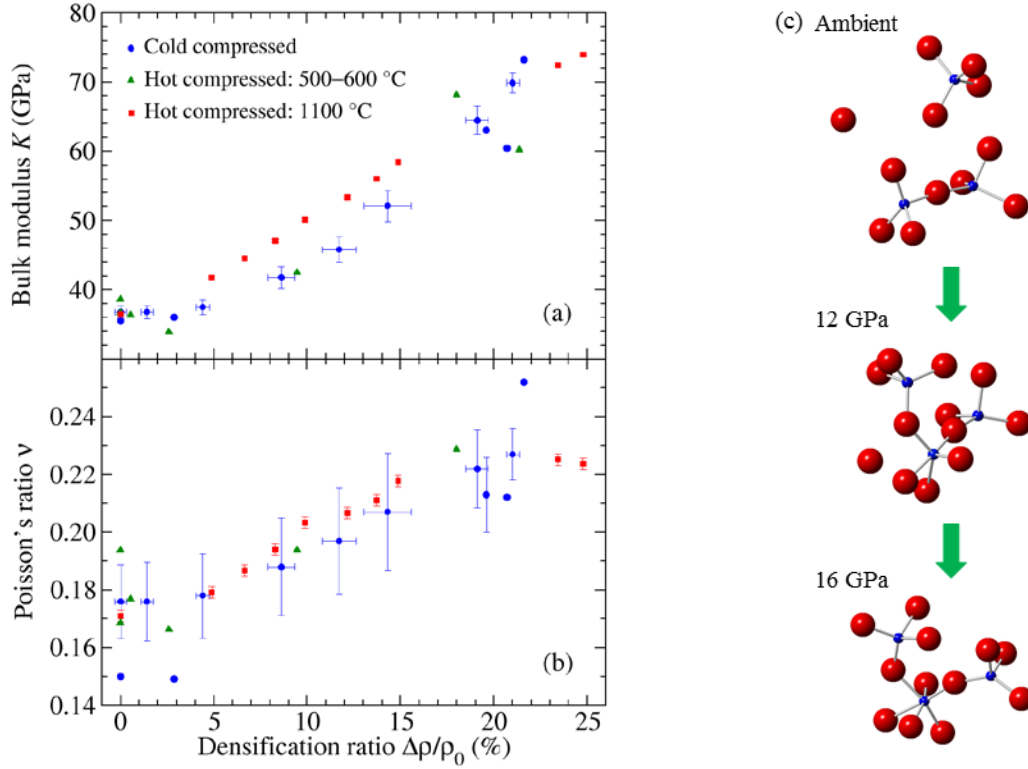
Figure 1. The (a) bulk modulus and (b) Poisson's ratio for SiO_2 glass versus the densification ratio $\Delta\rho/\rho_0 = (\rho - \rho_0)/\rho_0$, where ρ and ρ_0 are the densities of the compacted and normally-prepared glass, respectively. These properties depend on the extent of densification, and may also depend on the route taken to densification, e.g., cold compression at ambient temperature versus hot compression near the glass transition temperature ($\sim$1200 °C for SiO_2 at ambient pressure). The data sets originate from References 7 and 9. (c) Snapshots from a molecular dynamics simulation showing the pressure-driven change to the Si-O coordination number in SiO_2 glass at 300 K. The Si and O atoms are represented by the small blue and large red spheres, respectively.
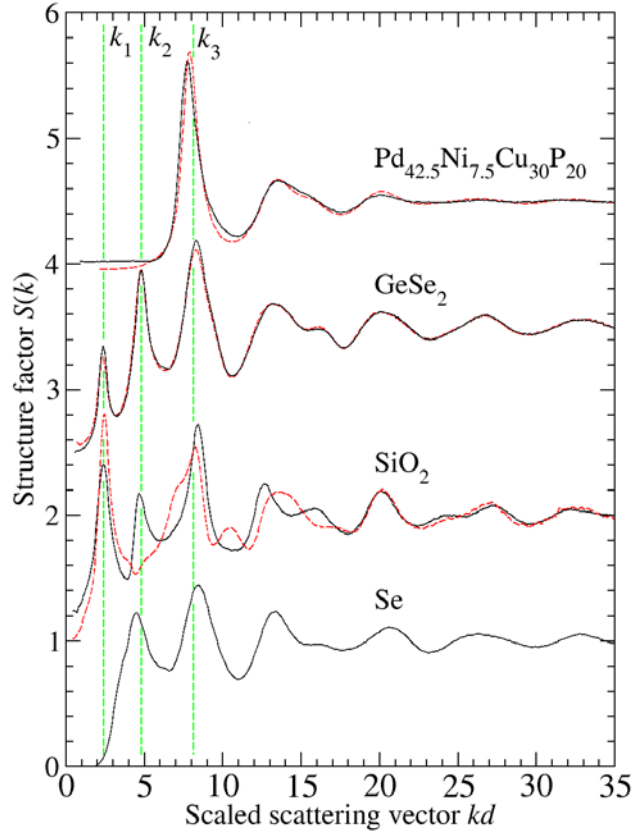
Figure 2. The structure factors $S(k)$ measured by neutron (solid curves) and x-ray (broken curves) diffraction at ambient pressure versus the scaled scattering vector kd. The structure factors are typical of those measured for a bulk metallic glass ($Pd_{42.5}Ni_{7.5}Cu_{30}P_{20}$), network-forming chalcogenide ($GeSe_2$) and oxide (SiO_2) glasses, and a chain-like polymeric glass (Se). Vertical broken lines indicate the approximate positions of the first three peaks for the network-forming materials. Taken from Reference 19. © American Physical Society.

How does pressure change the structure of glass on different length scales?

On quenching a glass-forming liquid at ambient pressure, the atoms will self-assemble to form a structure that depends on the nature of the interatomic interactions and quench rate. Ordering can occur on different real-space length scales, which leads to the appearance of peaks in the structure factor $S(k)$ measured by diffraction experiments (**Figure 2**), where k denotes the magnitude of the scattering vector. For network-forming glasses, three peaks generally occur with positions k_i ($i = 1$, 2, or 3) that scale roughly with the nearest-neighbour interatomic distance d, such that $k_1d \simeq 2 - 3$, $k_2d \simeq 4.6 - 4.9$ and $k_3d \simeq 7.7 - 8.9$.[19] Each peak is associated with real-space ordering of periodicity $2\pi/k_i$.[20] In a network glass such as SiO_2, the periodicities given by k_3, k_2 and k_1 are commensurate with the nearest-neighbour atomic separations, with the size of the network-forming SiO_4 motifs, and with the arrangement of these motifs on an intermediate range, respectively. In contrast, $S(k)$ for a metallic glass is often dominated by a first peak at a scaled peak position $k_3d \simeq 7 - 8$, which reflects a close-packed atomic structure.

In general, the structure of glass will respond to pressure on different length scales.[19] In the case of SiO_2 glass, for example, the tetrahedral SiO_4 units first reorganise in order to reduce the free volume, and the resultant compaction of the network registers itself on the intermediate length scale associated with k_1. Once the tetrahedral units are maximally packed, they commence their transformation into octahedral SiO_6 units, and there are concomitant changes to the value of k_2. This transformation of the network-forming motifs has a profound effect on the network connectivity (Figure 1c), thereby changing structure-related properties of the material such as its density, compressibility, elastic constants and ability to flow.

What controls the structural transformations in oxide glass?

Figure 3 shows that the pressure-induced transformation of the A-O coordination number $\bar{n}_{AO}$ for network-forming motifs (A = B, Si or Ge) can be rationalised in terms of the oxygen-packing fraction η_O for a variety of glassy and liquid oxides.[21] The η_O parameter gives the fraction of the available volume occupied by oxygen atoms. For instance, there is a plateau of stability for tetrahedral AO_4 units in SiO_2, GeO_2 and silicate materials that ends at $\eta_O \simeq 0.58$, within the range of packing fractions expected for a random loose-packing of equally-sized hard spheres, i.e., $\eta_{RLP} = 0.55 - 0.60$. All of the data sets show structures based on octahedral AO_6 units once $\eta_O \simeq 0.64$, which corresponds to the packing fraction found for a random close-packing of equally-sized hard spheres. There is a plateau of stability for these AO_6 units that extends to $\eta_O \simeq 0.72$, the packing fraction at which a further increase in $\bar{n}_{AO}$ occurs with pressure. The sensitivity of η_O to structural change can be understood on the basis of an ionic interaction model: O^{2-} ions have an ability to change both their size and shape in response to the coordination environment in which they are confined.[19,25]
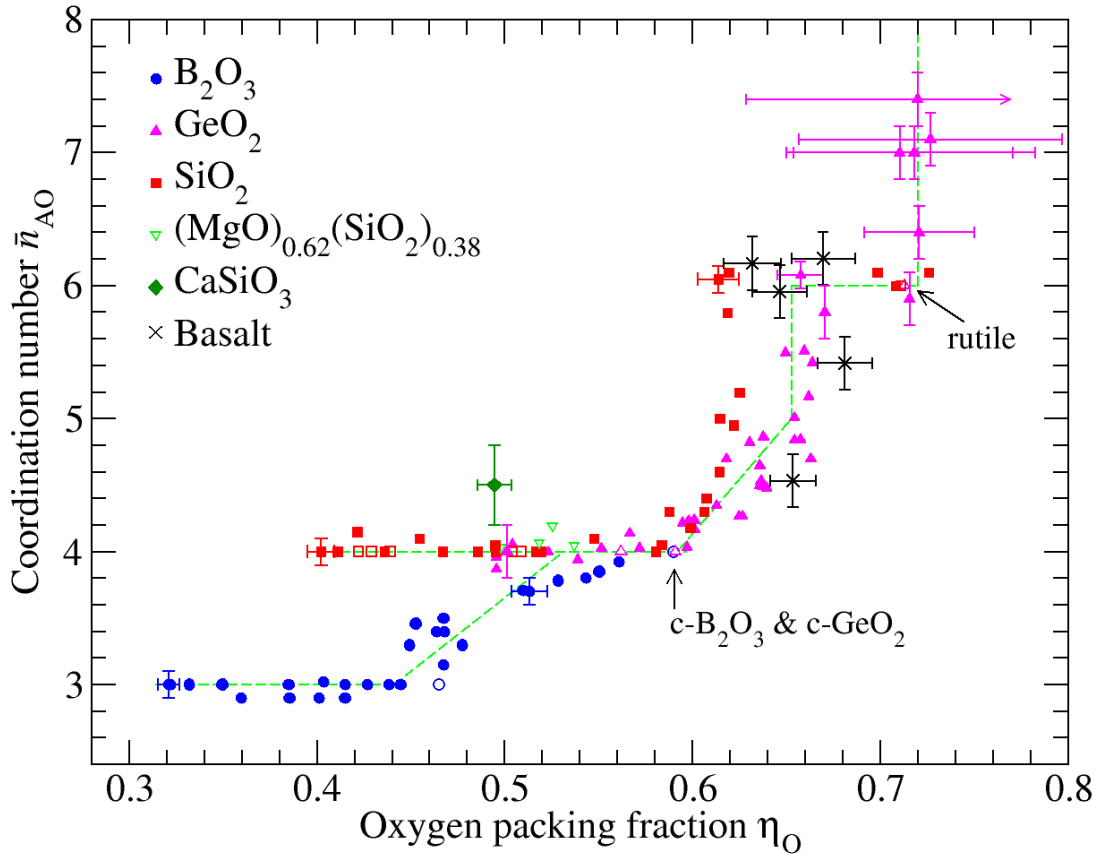
Figure 3. The A-O coordination number $\bar{n}_{AO}$ versus the oxygen-packing fraction η_O for glassy B_2O_3, GeO_2, SiO_2 and $(MgO)_{0.62}(SiO_2)_{0.38}$ under compression at room temperature and pressures up to 100 GPa. Data sets are also given for molten $CaSiO_3$ ($P = 6$ GPa, $T = 2130$ K),[22] molten basalt (an aluminosilicate) under deep mantle conditions ($P \leq 60$ GPa, $T = 2273–3273$ K),[23] and the room-temperature polymorphs of crystalline B_2O_3 (blue ○), SiO_2 (red □), and GeO_2 (magenta Δ). Adapted from References 12 and 21 to include the results of Kono et al.[24] for GeO_2 glass.

How does structural change affect the deformation of glass?

The cold-compression processes that occur under the tip of an indenter illustrate several of the effects of pressure on the structure and deformation of glass. In general, the indenter will cause both densification and volume conserving shear flow.[8,14,26] Even brittle glasses such as SiO_2 can flow if subjected to high enough loads, i.e., there is a brittle to ductile transition. The competition between densification and shear flow can be explored via molecular dynamics simulations of nano-indentation tests on normally-processed versus densified SiO_2 glass.[27] For the normally-processed glass (**Figure 4**), the indenter causes a large fractional change in the local density with little of the shear flow that leads to pileup of material at the glass surface. This behaviour is consistent with experiment[28] and reflects the low atomic-packing fraction of the material. In comparison, the densified glass shows a smaller fractional change in the local density, and shear flow leads to more extensive pileup of material at the glass surface and to residual shear strain in the pileup region. This behaviour

is also consistent with experiment.[14] The densified material has larger elastic moduli and an increased nano-hardness, where the latter measures the resistance of a solid to penetration or permanent deformation.
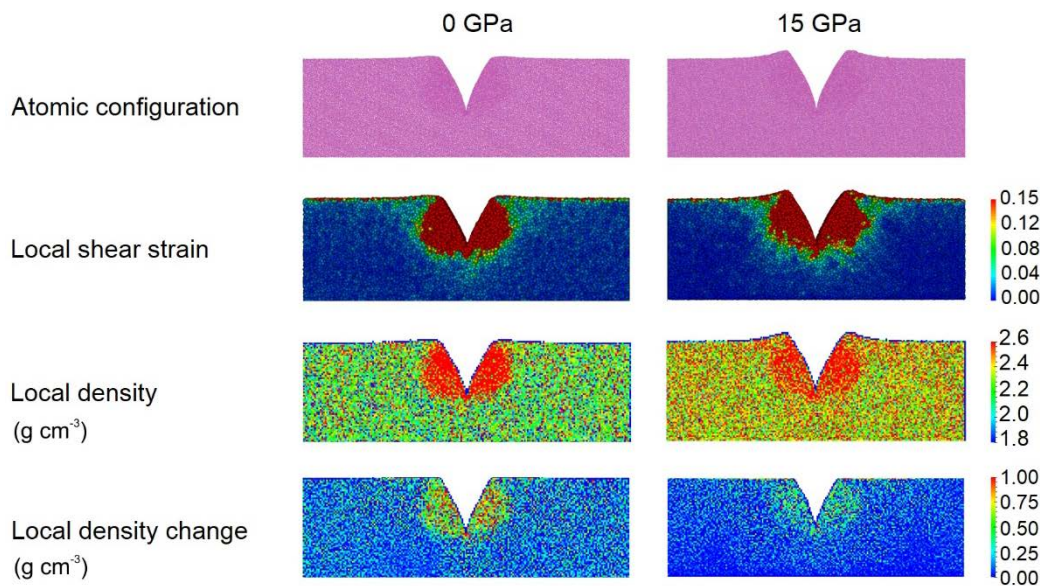

Figure 4. The atomic configurations, local shear strain, local density, and local density change after a nano-indentation test on normally-processed versus densified SiO_2 glass as obtained from molecular dynamics simulations using a V-shaped indenter. The densified glass was prepared from a liquid by quenching to room temperature at a pressure of 15 GPa. Adapted from Reference 27.

In the deformation of SiO_2 glass under cold compression, molecular dynamics simulations show that fivefold coordinated Si atoms appear as intermediaries in the transformation of tetrahedral SiO_4 to octahedral SiO_6 units.[27,29,30] At ~10 GPa, there is a minimum in the pressure-dependent yield-strength, i.e., the stress at which the material begins to deform plastically,[31] and the onset of plastic deformation means that permanently densified glass is recoverable from pressures above 10 GPa. The pressure-induced ability of Si atoms to adopt SiO_5 configurations enhances the capability for localised re-bonding and relaxation, thus facilitating plastic deformation via both the densification and shear-flow mechanisms.[27,29] Fivefold coordinated Si atoms also play a key role as intermediaries in the so-called "zipper" model for ring closure which accurately predicts the pressure dependence of the mean primitive ring size in SiO_2 glass under cold-compression, where a ring is deemed to be primitive if it cannot be decomposed into smaller rings,[30] and they are proposed as one of the possible transition states for the high-temperature growth of quartz from silica glass.[32]

Outlook

As compared to silica, less information is known about other glassy materials under pressure, especially when they comprise two or more components. It is important to address this issue in order to help in the development of new materials with the required characteristics via the principles of rational design,[33] e.g., through the adoption of machine learning methods.[34] In

addition, most experiments on glass structure have focused on the material response to near-hydrostatic conditions, so there is much to be learnt about the structural changes in glass under shear stress.[35] The behaviour of water in silicate glass is important because it has a profound effect on crack formation and propagation,[36] where the high-stress environment found at a crack tip is believed to aid in the dissociation of water molecules, thus severing bridging Si-O-Si connections by the formation of non-bridging Si-O-H groups.[37]

References

1. P.W. Bridgman, I. Šimon, *J. Appl. Phys.* **24**, 405 (1953).

2. J.D. Mackenzie, *J. Am. Ceram. Soc.* **46**, 461 (1963); **47**, 76 (1964).

3. H.M. Cohen, R. Roy, *Phys. Chem. Glasses* **6**, 149 (1965).

4. M. Grimsditch, *Phys. Rev. Lett.* **52**, 2379 (1984).

5. T. Grande, J.R. Holloway, P.F. McMillan, C.A. Angell, *Nature.* **369**, 43 (1994).

6. T. Rouxel, *J. Am. Ceram. Soc.* **90**, 3019 (2007).

7. T. Deschamps, J. Margueritat, C. Martinet, A. Mermet, B. Champagnon, *Sci. Rep.* **4**, 7193 (2014).

8. T. Rouxel, *Phil. Trans. R. Soc. Lond. A* **373**, 20140140 (2015).

9. M. Guerette, M.R. Ackerson, J. Thomas, F. Yuan, E.B. Watson, D. Walker, L. Huang, *Sci. Rep.* **5**, 15343 (2015).

10. V.V. Brazhkin, A.G. Lyapin, *J. Phys.: Condens. Matter* **15**, 6059 (2003).

11. D. Machon, F. Meersman, M.C. Wilding, M. Wilson, P.F. McMillan, *Prog. Mater. Sci.* **61**, 216 (2014).

12. P.S. Salmon, A. Zeidler, *J. Phys.: Condens. Matter* **27**, 133201 (2015).

13. S. Kohara, P.S. Salmon, *Adv. Phys. X* **1**, 640 (2016).

14. T. Rouxel, H. Ji, J.P. Guin, F. Augereau, R. Rufflé, *J. Appl. Phys.* **107**, 094903 (2010).

15. R. Gy, *Mater. Sci. Eng. B* **149**, 159 (2008).

16. A.K. Varshneya, *Int. J. Appl. Glass Sci.* **1**, 131 (2010).

17. J. Luo, P.J. Lezzi, K.D. Vargheese, A. Tandia, J.T. Harris, T.M. Gross, J.C. Mauro, *Front. Mater.* **3**, 52 (2016).

18. T. Rouxel, H. Ji, T. Hammouda, A. Moréac, *Phys. Rev. Lett.* **100**, 225501 (2008).

19. A. Zeidler, P.S. Salmon, *Phys. Rev. B* **93**, 214204 (2016).

20. P.S. Salmon, A. Zeidler, *Phys. Chem. Chem. Phys.* **15**, 15286 (2013).

21. A. Zeidler, P.S. Salmon, L.B. Skinner, *Proc. Natl. Acad. Sci. USA* **111**, 10045 (2014).

22. N. Funamori, S. Yamamoto, T. Yagi, T. Kikegawa, *J. Geophys. Res.* **109**, B03203 (2004).

23. C. Sanloup, J.W.E. Drewitt, Z. Konôpková, P. Dalladay-Simpson, D.M. Morton, N. Rai, W. van Westrenen, W. Morgenroth, *Nature* **503**, 104 (2013).

24. Y. Kono, C. Kenney-Benson, D. Ikuta, Y. Shibazaki, Y. Wang, G. Shen, *Proc. Natl. Acad. Sci. USA* **113**, 3436 (2016).

25. P.A. Madden, M. Wilson, *Chem. Soc. Rev.* **25**, 339 (1996).

26. T.M. Gross, *J. Non-Cryst. Solids* **358**, 3445 (2012).

27. F. Yuan, L. Huang, *Sci. Rep.* **4**, 5035 (2014).

28. S. Yoshida, J.-C. Sangleboeuf, T. Rouxel, *J. Mater. Res.* **20**, 3404 (2005).

29. Y. Liang, C.R. Miranda, S. Scandolo, *Phys. Rev. B* **75**, 024205 (2007).

30. A. Zeidler, K. Wezka, R.F. Rowlands, D.A.J. Whittaker, P.S. Salmon, A. Polidori, J.W.E. Drewitt, S. Klotz, H.E. Fischer, M.C. Wilding, C.L. Bull, M.G. Tucker, M. Wilson, *Phys. Rev. Lett.* **113**, 135501 (2014).

31. C. Meade. R. Jeanloz, *Science* **241**, 1072 (1988).

32. M.J. Aziz, S. Circone, C.B. Agee, *Nature* **390**, 596 (1997).

33. P.S. Salmon, *Nat. Mater.* **1**, 87 (2002).

34. J.C. Mauro, A. Tandia, K.D. Vargheese, Y.Z. Mauro, M.M. Smedskjaer, *Chem. Mater.* **28**, 4267 (2016).

35. D. Wakabayashi, N. Funamori, T. Sato, *Phys. Rev. B* **91**, 014106 (2015).

36. T.M. Gross, M. Tomozawa, *J. Non-Cryst. Solids* **354**, 5567 (2008).

37. T.A. Michalske, S.W. Freiman, *Nature* **295**, 511 (1982).